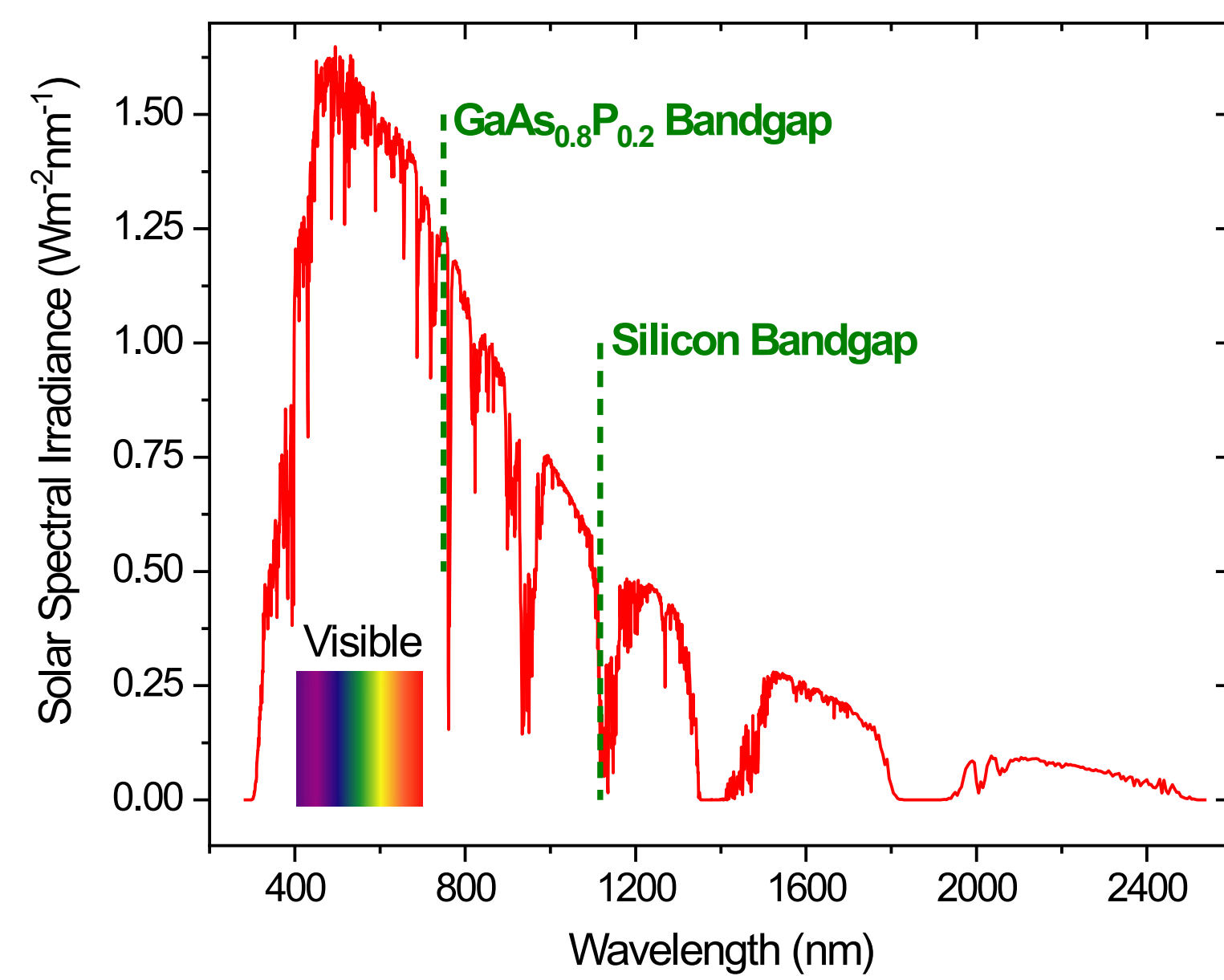
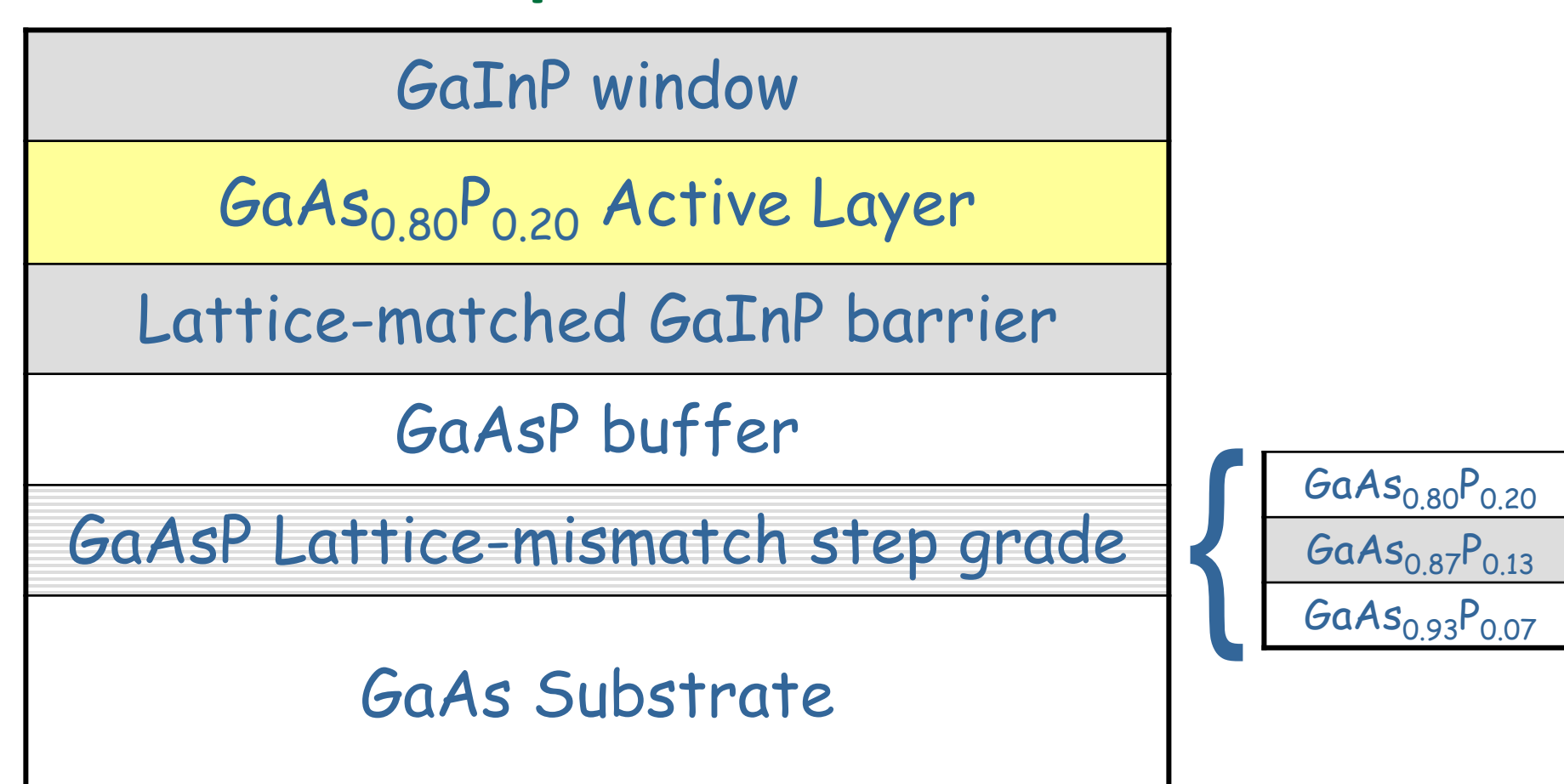


Motivation



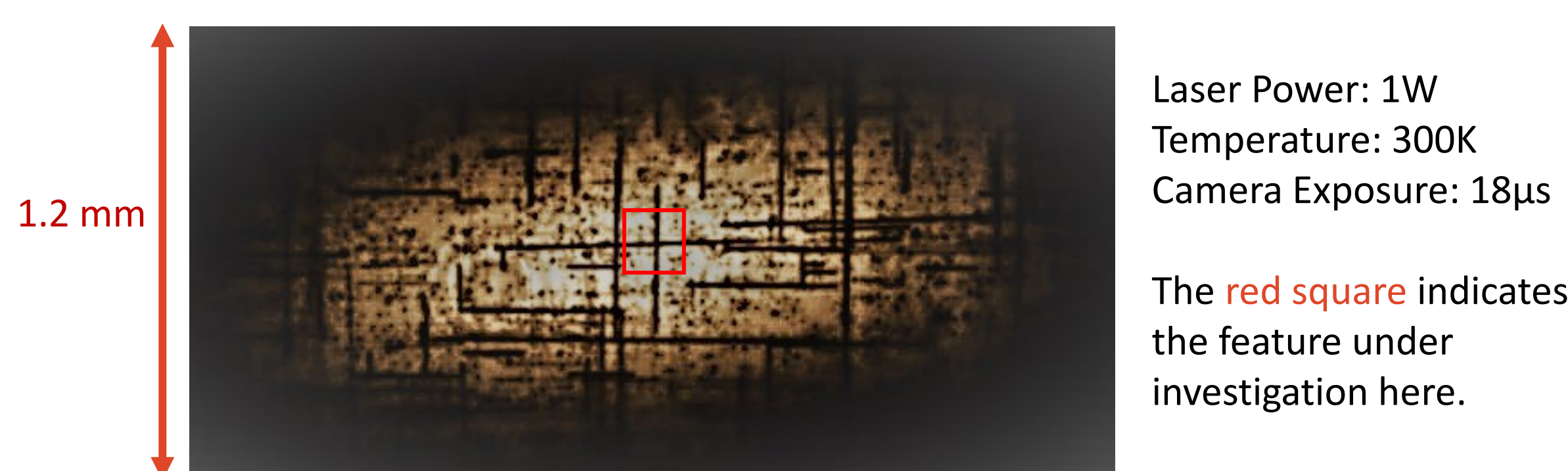
Metamorphic GaAsP on Silicon could improve the photovoltaic conversion efficiency of short wavelength sunlight.

Sample Structure



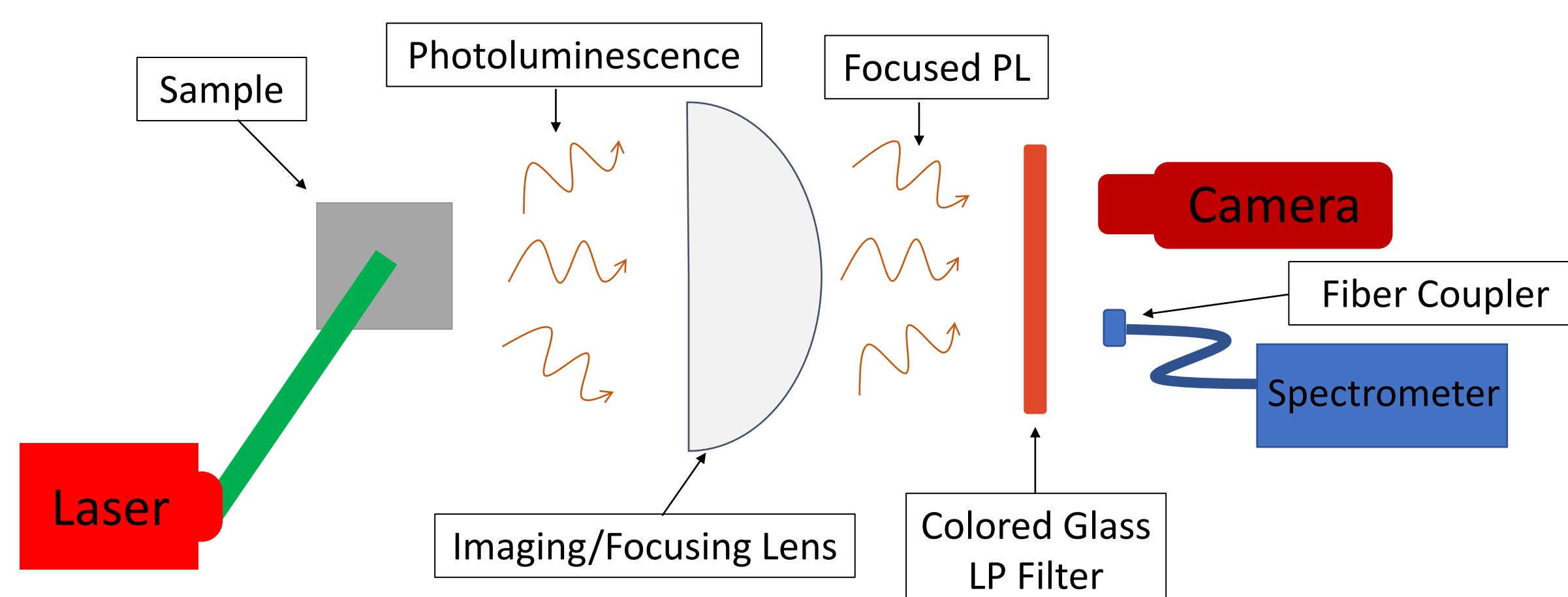
The test structure for this study is metamorphic GaAsP on GaAs.

Plan-View Photoluminescence Image

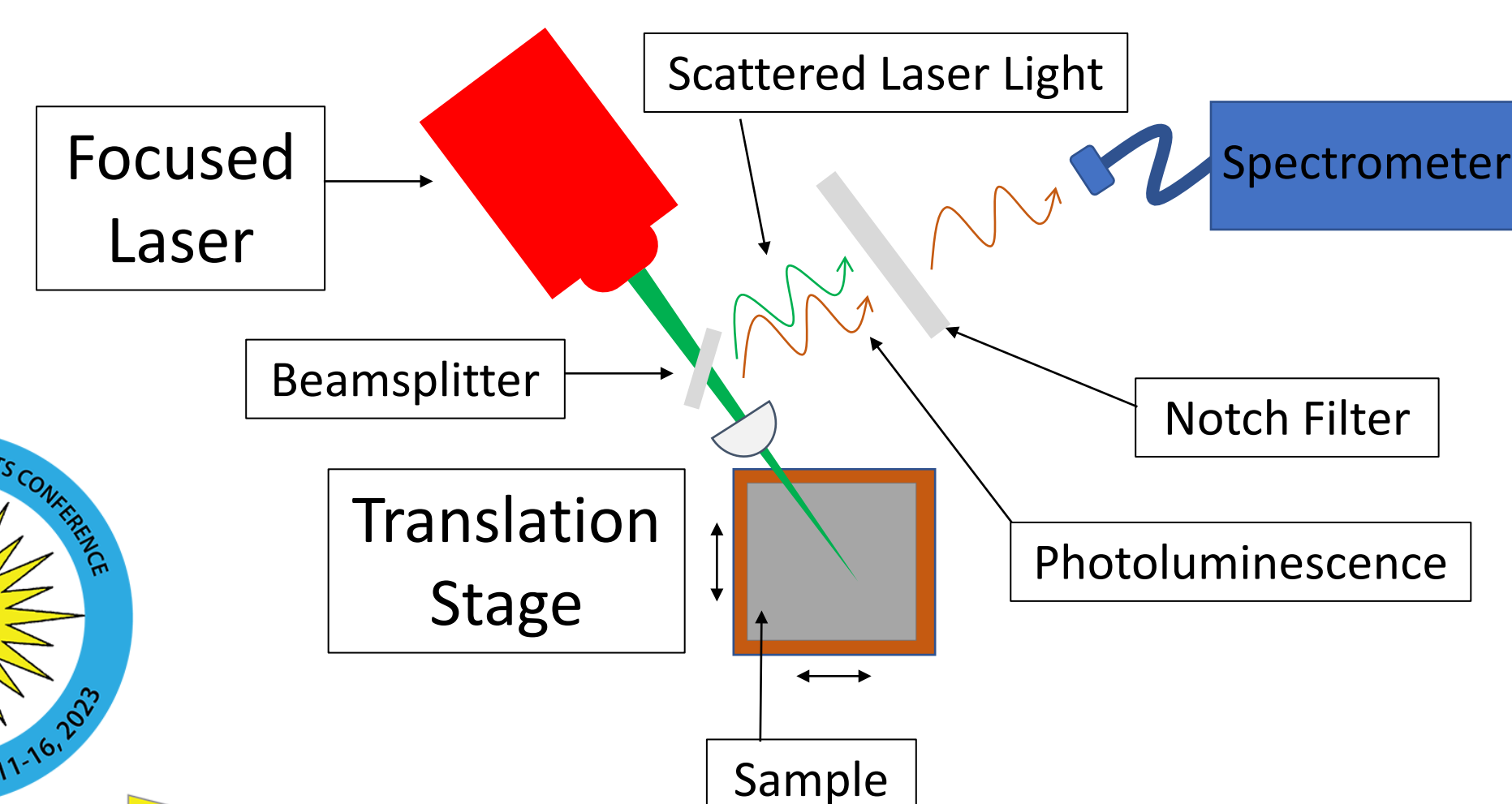


Photoluminescence (PL) images reveal dark crosshatch features where defect-related recombination limits optical emission.

Photoluminescence Imaging Experiment



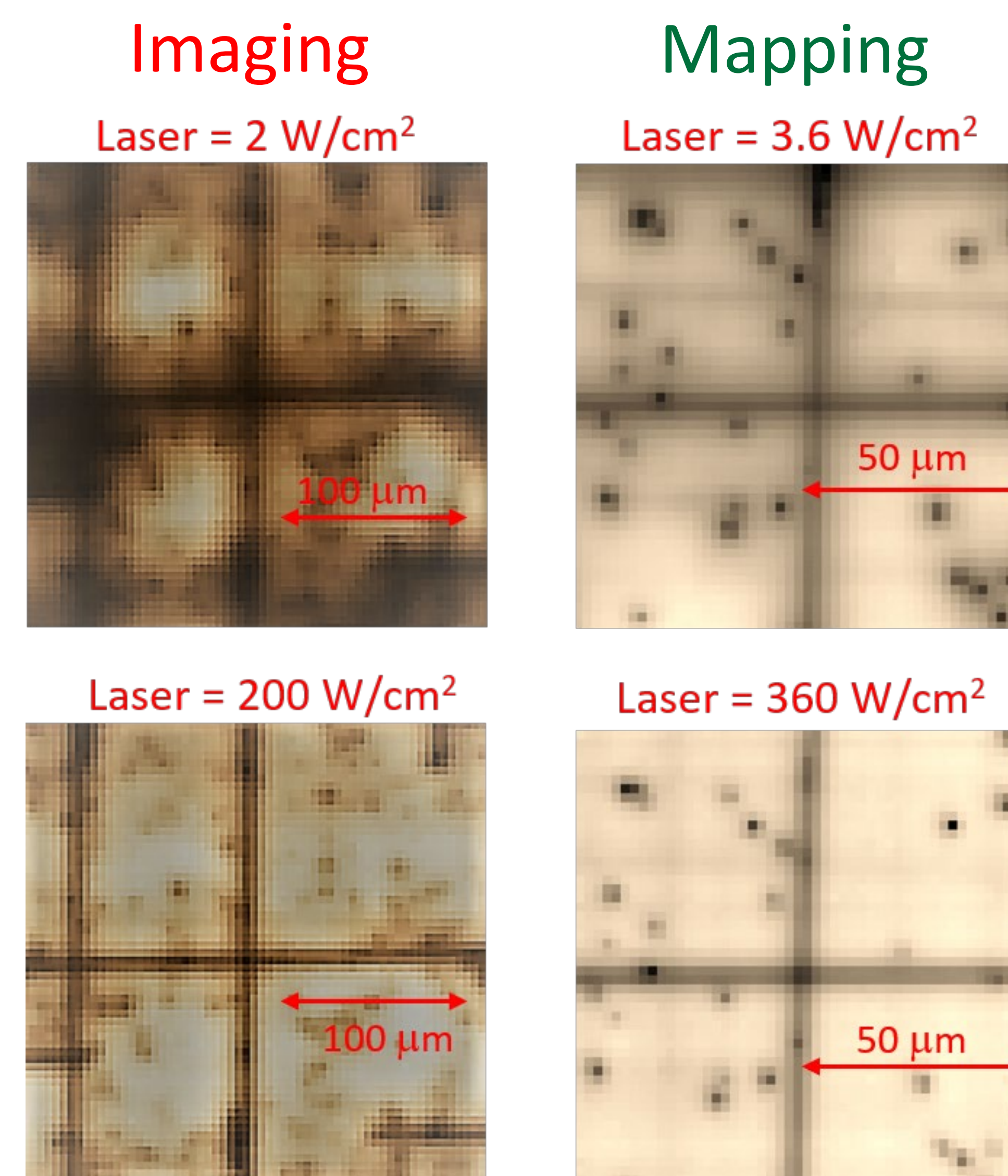
Confocal Mapping Experiment



Abstract

GaAsP alloys are good candidates for the upper junction in Si-based dual-junction tandem solar cells. However, monolithic growth of GaAsP on Si is limited by dislocation formation due to lattice mismatch. When metamorphic GaAsP is grown on GaAs substrates, dark crosshatch features can be observed in spatially-resolved electroluminescence and photoluminescence measurements. These features can be attributed to misfit dislocations in the epitaxial layers. We compare photo-luminescence imaging with complementary confocal mapping measurements to test models of diffusion and recombination near misfit dislocations in a GaAsP/GaInP heterostructure. The crosshatch features become sharper with increased photoexcitation in accordance with reduced lifetimes and diffusion distances. However, the imaging and mapping experiments require different defect-related recombination rates in our computational models.

Zoomed PL Images of Highlighted Feature



Note how defective features expand at low laser power where photoexcited carriers have longer lifetimes and diffusion lengths. Linear emission profiles were averaged to smooth out contributions from point defects.

Theoretical Model

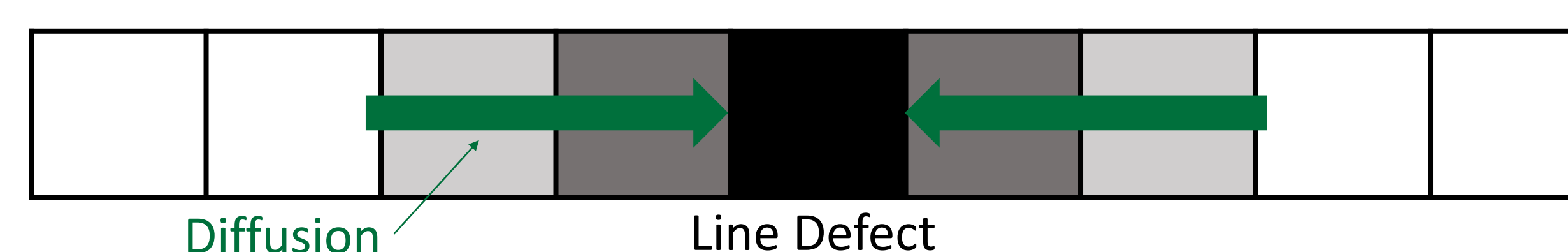
In steady-state, the local electron density does not change with time:

$$\frac{dn}{dt} = \text{Generation} - \text{Recombination} \pm \text{Diffusion} = 0$$

$$\frac{dn}{dt} = G - Bn^2 - An + J = 0 \text{ with } J = D(n_{\text{left}} + n_{\text{right}} - 2n)/w^2$$

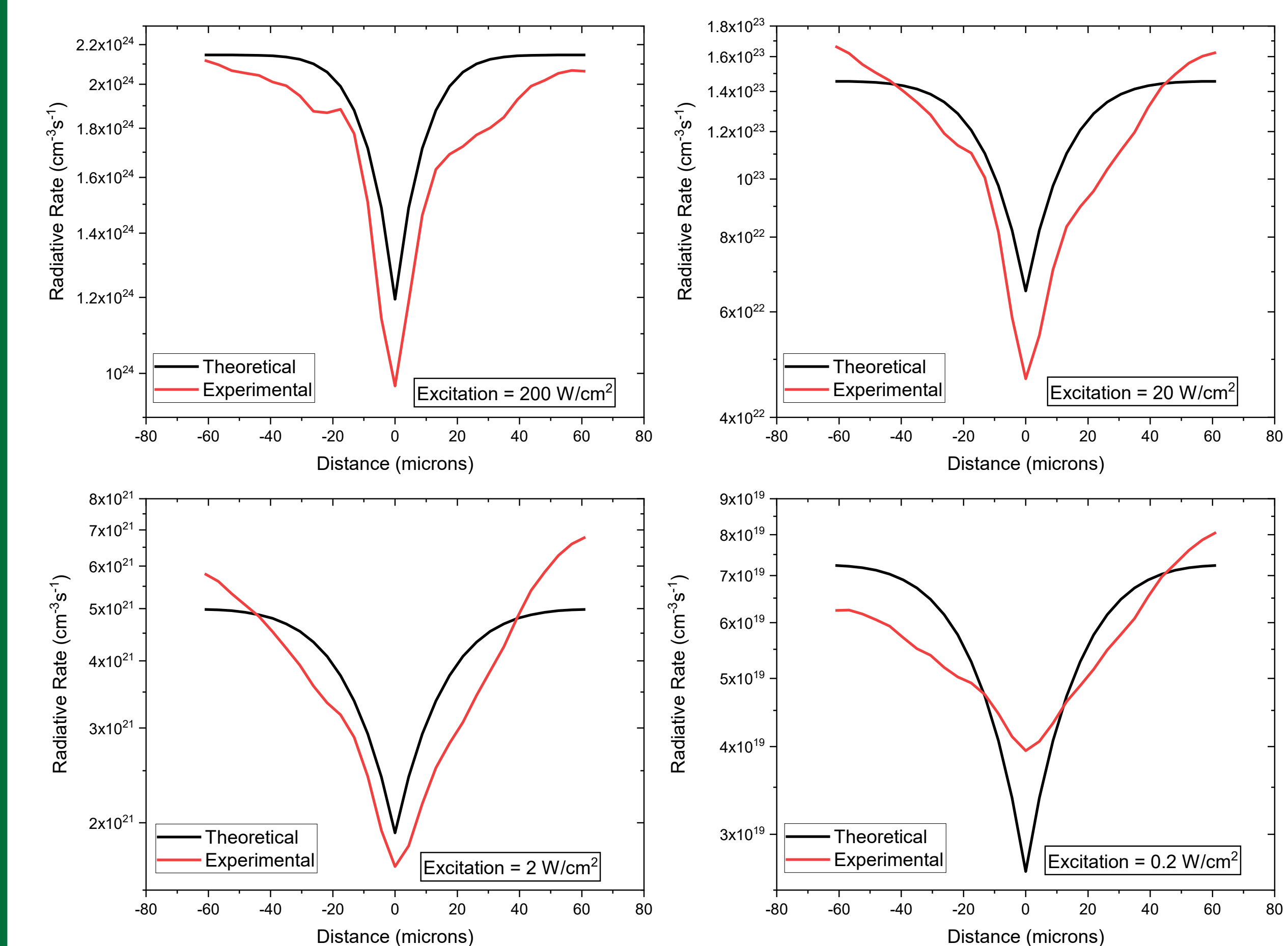
Computational Model

We assign a nonradiative recombination coefficient A_p to the non-defective pixels and $(A_p + A_L)$ to the pixel with the misfit dislocation. The augmented recombination in the defective pixel depletes carriers, driving diffusion towards the defect.



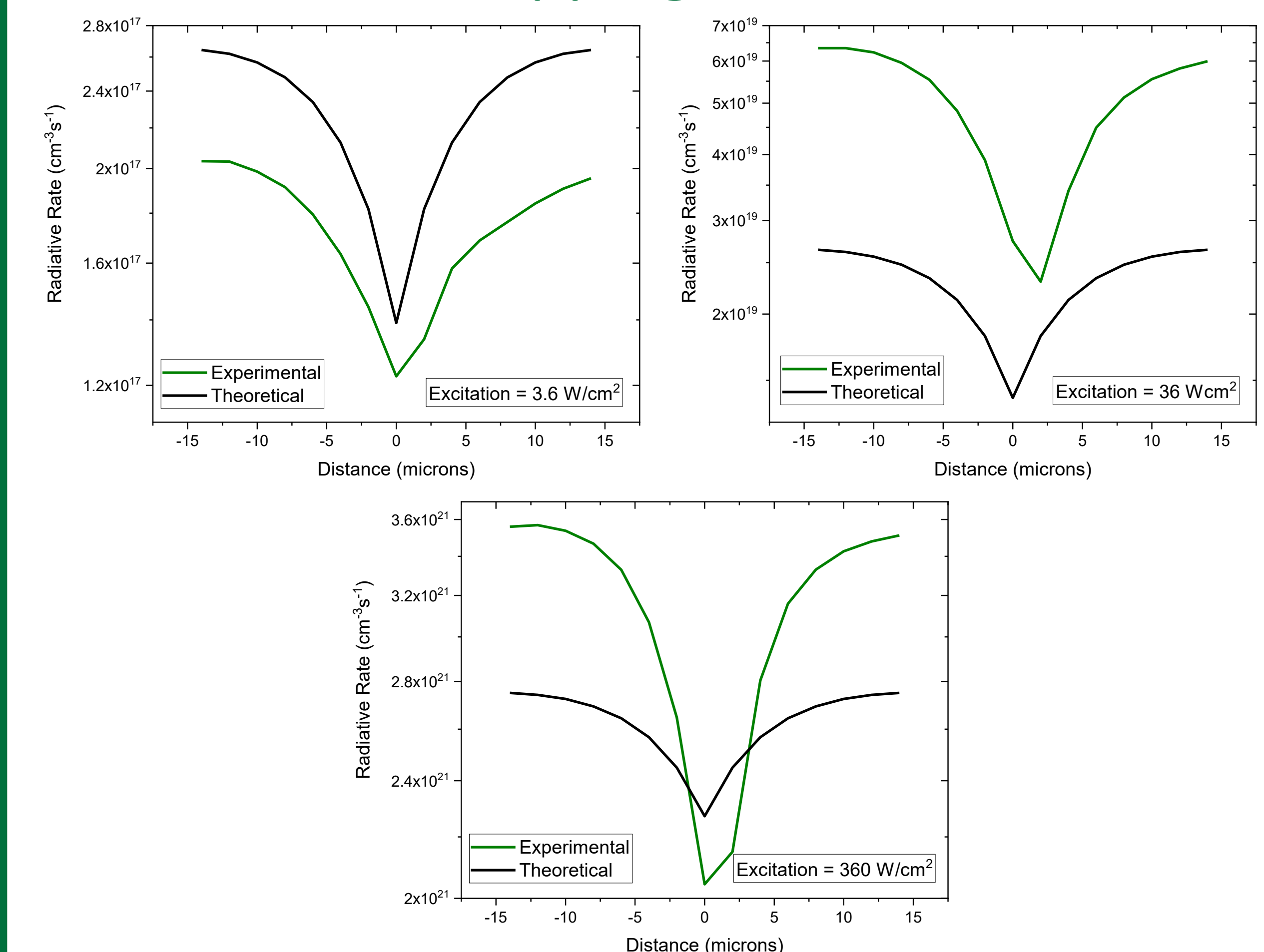
Our fitting algorithm iterates electron density calculations until the electron distribution reaches steady state. The program searches for SRH and acquisition-related Loss Factor (LF) parameters that best match our experimental results. Since the experiments and computational algorithms are different, we fit them separately.

Imaging Results



PL imaging and confocal mapping line profiles of the horizontal line defect under different photoexcitation conditions, showing how the radiative emission varies with distance from the misfit dislocation.

Mapping Results



Computational Fitting Parameters

Parameter	Experiment	
	Imaging	Mapping
B	$2 \times 10^{-10} \text{ cm}^3 \text{ s}^{-1}$	
D	$1 \times 10^2 \text{ cm}^2 \text{ s}^{-1}$	
LF	2700	0.51
A_p	$4.2 \times 10^6 \text{ s}^{-1}$	$1.2 \times 10^8 \text{ s}^{-1}$
A_L	$1.4 \times 10^8 \text{ s}^{-1}$	$4.5 \times 10^8 \text{ s}^{-1}$

Differing pixel dimensions bring the A_L coefficients near agreement, but the deduced A_p values are inconsistent. The role of diffusion is dramatically different in these experiments, but the discrepancy may also be due to limitations of the ABC recombination model over such a wide range of photoexcited carrier densities.

Acknowledgement

The work at UNCC was supported by ARO/Electronics (Grant No. W911NF-16-1-0263).